



## Synthesis, characterization of the valuable Hydroxysodalite and its application for remediation of toxic dye: Rhodamine B

Panmei Gaijon, M. Ramananda Singh, Sudipta Ghosh and Arun Kant\*

Department of Chemistry, Kirori Mal College, University of Delhi, Delhi 110007, India

### Abstract

Synthesis of valuable Hydroxysodalite (HsL) from the waste fly ash by using open hydrothermal method. Synthesized HsL was characterized using Fourier Transform Infrared spectroscopy, X-ray diffraction, Thermogravimetric analysis, Transmission Electron and Scanning Electron Microscopies. HsL was applied for remediation of toxic dye, Rhodamine B (RhB) from aqueous solution through method of adsorption. The batch adsorption study such as effect of pH, contact time and effect of concentration on adsorption of RhB on synthesized HsL was conducted to determine saturation adsorption condition. After adsorption of RhB on Synthesized HsL were also characterized using Fourier Transform Infrared spectroscopy, X-ray diffraction and Scanning Electron Microscopies. Pseudo second order kinetics and Langmuir adsorption isotherm was well fitted in case of remediation of RhB. Synthesized HsL have shown more uptake efficiency of RhB dye, which is about  $1032.5 \mu\text{g g}^{-1}$  of HsL at pH 8. Therefore, Synthesized HsL is considered to be efficient and economical adsorbent material for the remediation of RhB.

**Key words:** Hydroxysodalite, adsorption, kinetics, Fly ash, isotherms.

### Introduction

Hydroxysodalite (HsL) is a microporous aluminosilicate possesses significant physio-chemical properties, which are used as molecular sieving, adsorbent material, catalysis and as ion exchange. In this study the HsL ( $\text{Na}_8[\text{AlSiO}_4]_6(\text{OH})_2 \cdot 2\text{H}_2\text{O}$ ) was prepared by open hydrothermal method from waste fly ash [1]. HsL is a naturally occurring mineral have flexible structure and geometry that can accommodate variety of cation and have various application such as water softener, as adsorbent, as filler in paint and detergent binder [2-5]. HsL consists of aluminosilicate cage with sodium ion in inter-framework to form a cage structure like zeolite and each unit cell have four  $\beta$ -cage structures [6].

It has molecular sieving effect, adsorption capacity for variety of substances like volatile organic chemical, separation of isomers and mixture of gases, molecular sieving and they are thermally

stable up to high temperature of 1000°C [7-11]. The synthetic zeolites are painstaking as competitors for natural zeolite. Synthetic HsL from fly ash has many advantages over natural occurring HsL in terms of adsorption capacity and higher ion affinity [12,13].

Fly ash is fine powdered containing alumina and silica material which was produced by coal combustion have Ca, Na, Fe, Al, Mg as predominant elements with Cr, Ni, As, Hg, Ba, Zn, Se, as toxic metals [14, 15]. Heavy metal in the fly ash create pollutants in soil and has deleterious effect on natural aqueous body as well as human health during landfill and storage [16, 17].

Approximately 500 million tons of fly ash are produced throughout the year [18]. Fly ash generation is expected to increase in near future as the demand for electricity increases over years [19, 20]. Fly ashes are abundantly available and according to an estimate, about 125 million ton is generated per year and it will reach 200 million tons in India in coming days and 6.8 million tons in Malaysia [21, 22]. Production of Fly ash per year of different countries such as India, China, USA, Germany, UK, Australia and Canada are 112, 100, 75, 40, 15, 10 and 6 million tons respectively [17, 23] (Fig. 1b). Since coal is used as the major source of energy, it produces huge amount of fly ash annually [24, 25]. Now a days, fly ash is utilized in preparation of concrete in construction of building and the construction industry produces more than 10 billion tons of concrete annually [26, 27].

Utilization of Fly ash in percentage per year across various countries like India, China, USA, Germany, UK, Australia and Canada are 38, 45, 65, 85, 50, 45 and 75 respectively [28, 29], (Fig. 1c). More than 80% of the fly ash is disposed as in landfill and ponds, which causes the pollution to atmosphere leading to health problem to living beings [30] (Fig. 1a).

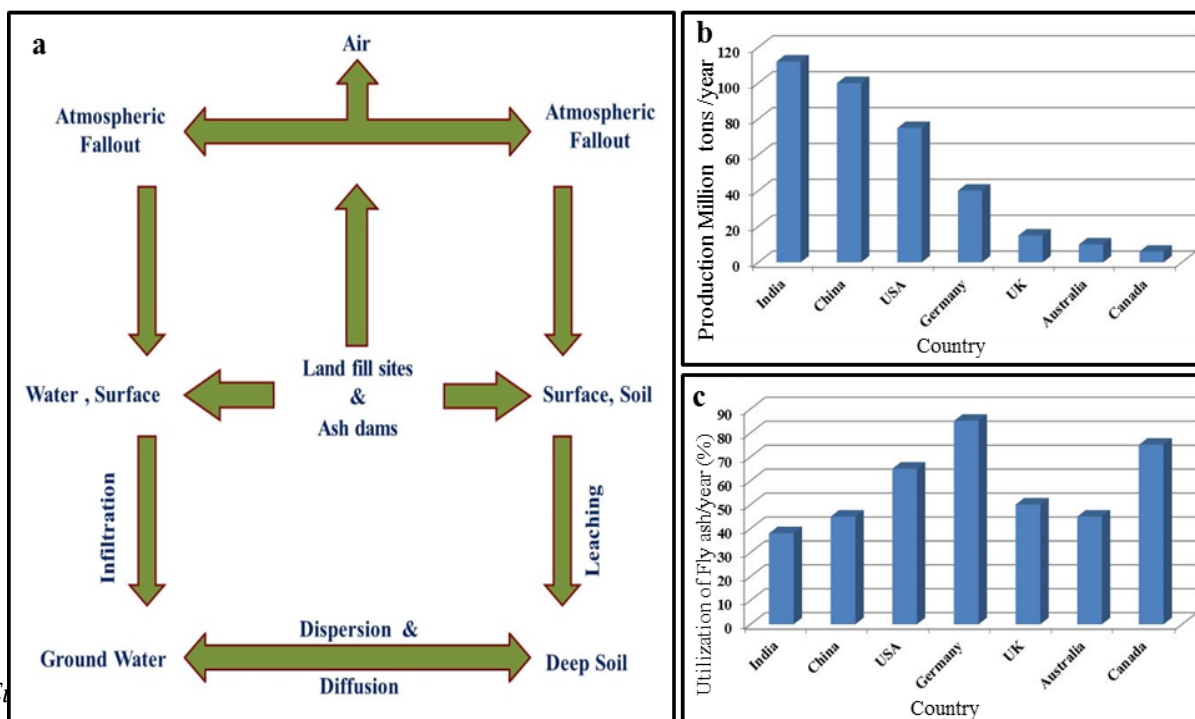


**Fig.1.** Schematic diagram showing (a) pathways of movement of Fly ash and causing of pollution (b) Globe use of Fly ash per year (c) Globe Production of Fly ash per year

Due to hazardous effect, high production and less utilization of fly ash, it is essentially required to convert the waste fly ash into the nonhazardous valuable product. Different techniques were in application for conversion of waste fly ash to useful materials, that are organic templates depending upon desired shape, structures, pore size of zeolite which contains silica (45-65%), alumina (25-40%) with some amount of heavy metal oxides [31-33]. This will reduce the disposal problem of fly ash and will help us to save our nature from variety of pollution associated with fly ash.

The synthesized HsL was tested for its application in remediation of Dye from aqueous solution. Dyes are widely used in the 21<sup>st</sup> century for various devotions to impart the color into different substances, such as papers, textiles, cosmetics, drugs, color coding, plastic, painting materials etc. [34]. Most of the dyes are organic molecule which is easily soluble in water that leads to the pollution of water bodies and affects the ecosystem. The effluents from the leather and textile industries were drained out into the natural water bodies, leading to the accumulation of dye materials, which are non-biodegradable organic materials.

The synthetic dyes are majorly health hazard in nature and it is also difficult to regenerate the dissolved oxygen in water bodies once it is polluted with dyes [35]. Because of above reasons, remediation of dyes molecules is paramount important. There are various methods using for remediation of dyes such as adsorption, precipitation, electro-kinetics coagulation, reverse osmosis, photo oxidation that are usually applied for the detoxification of dye molecule present in the wastewater. Out of them adsorption method is considered to be simple and economically viable for the remediation of toxic dye from waste water. A variety of adsorbent material such as biodegradable waste, naturally occurring clay material, carbon nanotubes, metal organo-framework, nano-metal oxides and agricultural waste are utilized in extraction of dyes etc. [36]. In the present work, synthesized HsL was applied for remediation of RhB dye. This dye is fluorescent, cationic in nature that used in textile as colorant, in foodstuffs and in pharmaceutical industries [37]. RhB is neurotoxic in nature for human as well as animal or other living being and

it also causes skin and eye damage and gene mutation too [38]. Since RhB dye are not degradable in the pH range of 6 to 8 and the most polluted water resources also have this pH range [39].

## **Experimental**

### **Materials**

Sodium Hydroxide, AR grade was purchased from Merck private limited Germany. Fly ash was collected from the National thermal power plant NTPC (India). Organic Dye Rhodamine B is cationic dye. C.I. Number C754170, molecular weight 479.02 and molecular formula  $C_{28}H_{31}ClN_2O_3$  was purchased from Merck private limited. HCl, KCl, NaOH and  $KH_2PO_4$  was procured from Thomas Baker Pvt. Ltd. Other analytical grade chemicals/reagents were used without any purification. All the reactions were done in double distilled water.

### **Technique**

Power X-ray diffraction (PXRD) pattern were recorded between 2 to 70° (2θ) with X-ray Diffractometer (D8 DISCOVER BRUKER AXS, Germany) at 40kV and 30mA. Fourier Transform Infrared spectroscopic (FTIR) study was conducted by Spectrum RXI Mid IR Perkin Elmer. Thermogravimetric analysis (TGA) was recorded using Perkin-Elmer system and Transmission Electron Microscopic assessment (TEM) was performed using TECNAI G2T30FEL and Scanning Electron Microscopic (SEM) analysis by using JEOL JSM-6610LV.

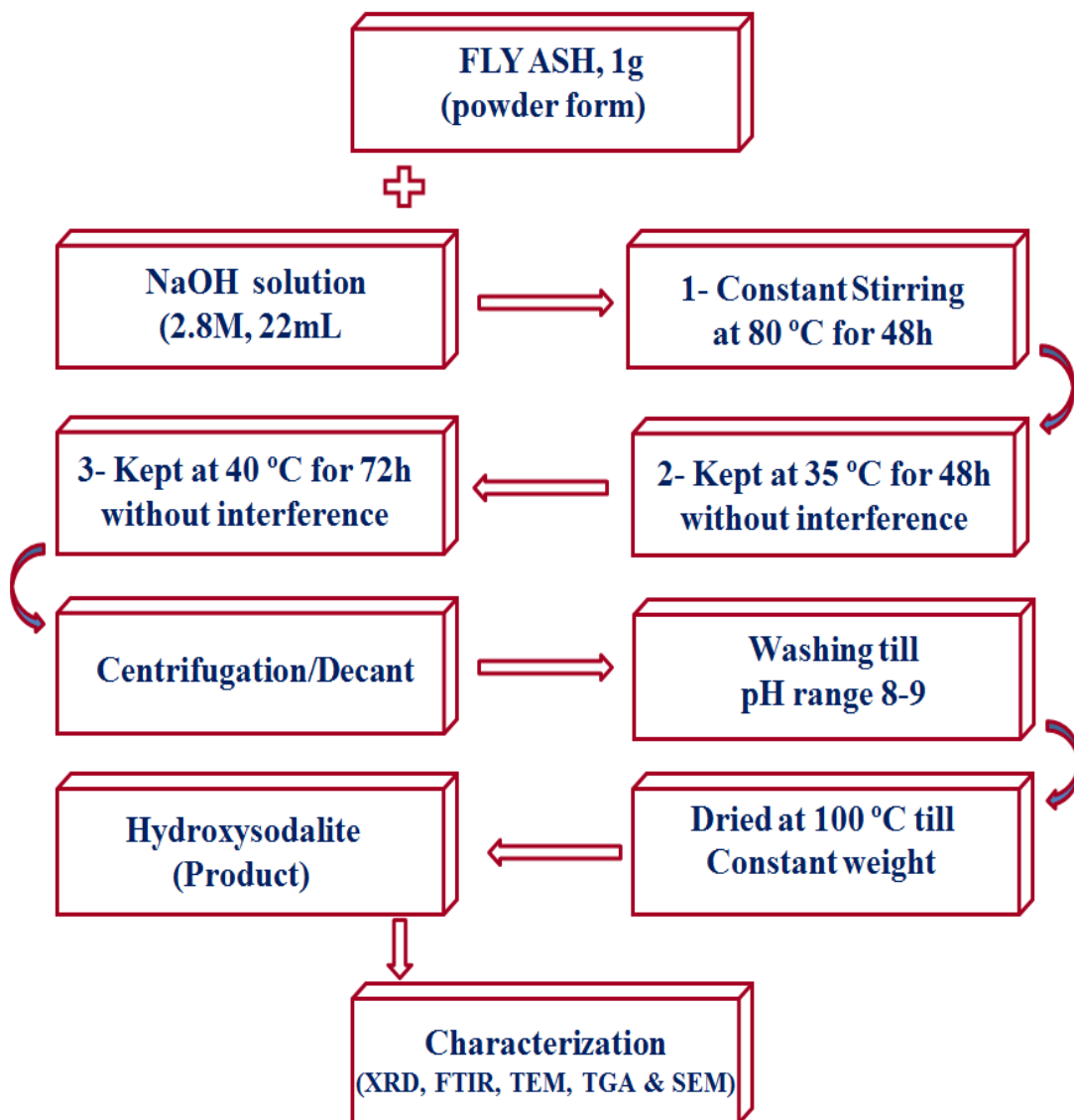
### **Synthesis of Hydroxysodalite**

Fly ash was used as the constituent of alumina (25-40%) as well as silica (45-65%) for preparation of framework aluminosilicates (Hydroxysodalite). HsL has three-dimensional open crystal structures, variable pore size (Fig. 2).



fig. 2. Two dimensional Structure of Hydroxysodalite

They are more hydrophilic in nature. The HsL was synthesized through two step hydrothermal technique. 1 (one)g of fly ash was first taken in a 100 ml conical flask and 22ml of 2.8M NaOH solution was added into it. The reaction mixture was maintained at 80°C with constant stirring on a magnetic stirrer for 48 h by open hydrothermal process, a suspension of brownish color was obtained. Then, reaction mixture was further kept at 35°C for 48 hrs. and at 40 °C for 72 hrs. without interference.



Scheme 1. Schematic representation of methodology for synthesis and characterization of HsL

The supernatant was decanted from the reaction mixture. The residue product was washed with double distilled water several times till the filtrate's pH becomes neutral. The precipitate obtained was dried at 100 °C in an oven to have constant weight. The synthesized product was characterized by standard characterization techniques as represented in Scheme 1.

## **Result and discussion**

### **Estimation of RhB dye in solution**

Adsorption studies of RhB dye on synthesized Hydroxysodalite was performed with variation of pH of RhB dye solution to show its effect on adsorption, contact time for batch adsorption as well as concentration of the RhB solution. Percentage adsorption of RhB dye on the HsL was calculated by using following equation.

$$\% \text{ Adsorption of dye} = \frac{\text{Initial concentration of dye} - \text{Final concentration of dye}}{\text{Initial concentration of dye}} \times 100$$

### **Calibration plot for quantitative assessment of RhB dye**

A 250 ppm solution of RhB dye was made in a 500 mL volumetric flask as a stock solution and subsequently the solutions of 1, 2, 3, 4, 5 ppm were made through dilution from the stock solution. The absorbance value was recorded for each of the solution and the calibration plot was prepared with adsorption versus concentration for further calculation that involved in the experiment. Accordingly, the  $\lambda_{\text{max}}$  of RhB dye was found to be at 556 nm (Fig 3a) in the aqueous solution. Since RhB dye in aqueous solution is more stable in pH range of 4 to 12 due to this all the estimation of dye by UV-Visible spectroscopy was performed at pH 7 [39,40].

### **Batch adsorption Studies with HsL**

In Batch adsorption studies, pH effect of dye solution on adsorption of RhB on synthesized HsL was tested. Twelve set of conical flask, each have 25 ml of 25 ppm of RhB solution having pH of 1 to 12 with constant concentration was allowed to interact with 20 mg of HsL for 10 minutes. The percentage adsorption/uptake was measured as a function of pH of solution and percentage uptake at pH 1 and pH 5 were found to be 75.64 and 77.21 respectively. The highest percentage adsorption of 82.3 % was found at pH 8 depicted in Fig 3b. In the basic medium HsL is stable

and adsorptive site of adsorbent is more active. Accordingly, pH 8 was chosen for further estimation of RhB with different studies.

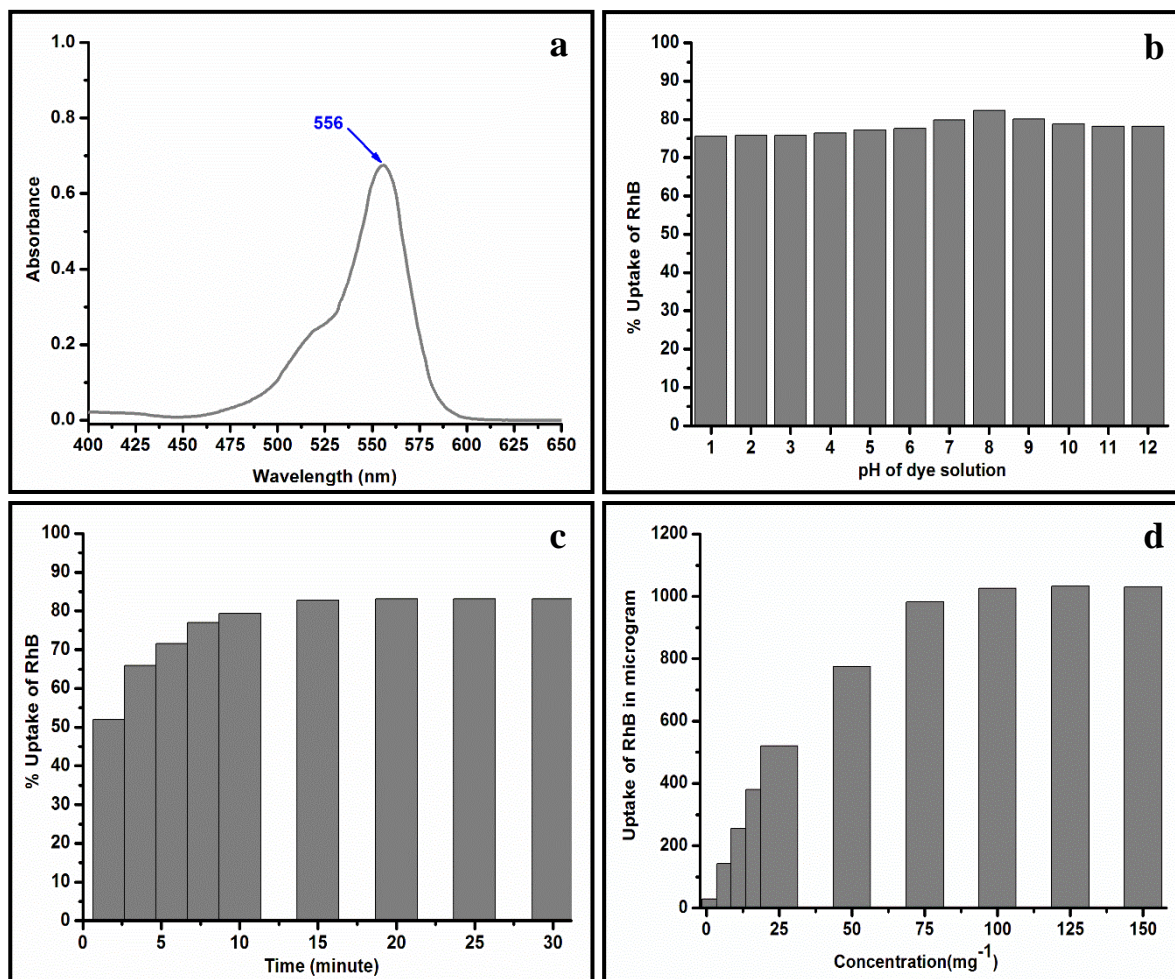


**Fig.3.**(a) Absorbance value of RhB dye (b) % Uptake of RhB as function of pH (c)%Uptake of Dye as function of contact time (d) Uptake of RhB as function of its concentration

In case of percentage adsorption /uptake as a function of contact time, in which time used to take 2, 4, 6, 8, 10, 15, 20 25 minute interval and performed up to 30 minutes(Fig 3c). Percentage adsorption of dye is very fast and was found to be 51.96 within 2 minutes and it increases up to 83.14 in 20 minutes, and it becomes saturated after 20 minutes due to all vacant adsorptive sites being filled on synthesized HsL. This contact time i.e.; 20 minutes and pH 8 was accordingly decided for further adsorption studies. After that we have studied Percentage

adsorption of RhB dye as a function of concentration in which took different concentrations of RhB dye solution such as 5 ppm, 10 ppm, 15 ppm, 20 ppm, 25 ppm, 50 ppm, 75 ppm, 100 ppm, 125 ppm, 150 ppm (Fig 3d) at pH 8 and for saturation time 20 minutes with 20 mg of HsL. Percentage adsorption/Uptake of RhB dye was found to be 141.91  $\mu\text{g}$  and 775.74  $\mu\text{g}$  at 10 ppm and 50 ppm, respectively. The highest uptake of 1032.48  $\mu\text{g}$  was found at 125 ppm concentration of RhB. This composition was characterized by various techniques for interpretation of interaction between synthesized HsL with RhB dye molecule.

### Adsorption Isotherm studies

Adsorption isotherm is a mathematical model which describes the distribution of adsorbate molecule among the adsorbent and liquids. Based on assumptions and homogeneity/heterogeneity of the adsorbents, the possible nature of interaction between adsorbates and adsorbent molecule was explained. Langmuir and Freundlich adsorption isotherm model were discussed in adsorption isotherm studies [41-46].

Freundlich isotherm model explains about the importance properties of the heterogeneous surface, reversible adsorption and formation of more than two layers on adsorbent surface. Equation 1 is the linear equation of Freundlich adsorption isotherm model. The Plot of  $\log q_e$  versus  $\log C_e$  was linear with the slope of  $1/n$  and  $K_f$ , the intercept (Fig 4b). The value of slope ( $1/n$ ) indicates strength of adsorption process that is,  $1/n < 1$  is indicative of normal adsorption and  $1/n > 1$  indicates the cooperative adsorption. When  $1/n = 1$ , it means independent concentration that is partitioned between two phases.

$$\text{Log } q_e = \log K_f + 1/n \log C_e \quad (\text{Equation 1})$$

Langmuir adsorption isotherm model gives the idea of mono layer formation adsorbent surface. Equation 2 is the linear form of Langmuir adsorption isotherm. Plot between  $\log C_e/q_e$  versus  $\log C_e$  gives the linear (Fig 4a). In this equation, the capacity of adsorbent (mg/g) is represented by  $q_{\text{max}}$  and the adsorption constant ( $\text{dm}^3/\text{mg}$ ) by  $K_L$ , its slope by  $1/q_{\text{max}}$  and the intercept by  $1/(q_{\text{max}} K_L)$ . Separation factor referred to the Langmuir is represented by  $R_L$  defined by Webber [47] which is represented in Equation 3.

Magnitude of  $R_L$  indicates relative affinity between the both adsorbates and adsorbents. The phenomenon of adsorption was obtained from  $R_L$  values. If  $R_L$  value is equal to 1, which



indicates linear, the favorable adsorption is indicated by the value of  $R_L$  between 0 to 1 and the value of  $R_L$  greater than 1 represents unfavorable adsorption.

When it is equal to zero, it indicates irreversible adsorption.  $R_L$  values are calculated at all the possible concentration and its value less than one indicates favorable adsorption, the plot between  $R_L$  versus concentration (Fig.5d).

$$C_e/q_e = 1/(q_{\max}K_L) + C_e/q_{\max} \text{ (Equation 2)}$$

$$R_L = 1/(1 + K_L C_i) \text{ (Equation 3)}$$

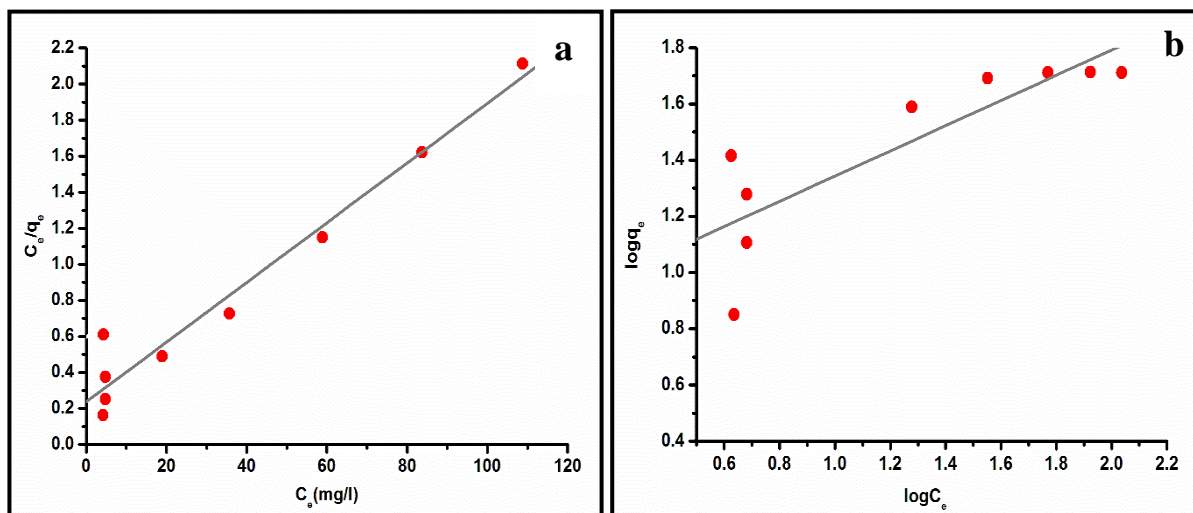


**Fig.4.**(a) Langmuir Adsorption isotherm and (b) Freundlich Adsorption isotherm

The Langmuir and Freundlich's constant parameters were arranged in Table 1. The best fitted isotherm was indicated by the correlation coefficient ( $R^2$ ) of the plots. Since  $R^2 = 0.9596$  in Langmuir isotherm in comparison to Freundlich isotherm where its  $R^2 = 0.7254$ , so, it follows Langmuir adsorption isotherm model.

**Table 1.** Parameters constant of Freundlich Adsorption isotherm and Langmuir Adsorption isotherm

Freundlich isotherm constants				Langmuir isotherm constants			
1/n	n	$K_f$ ( $\text{mg g}^{-1}$ )	$R^2$	$q_{\max}$ ( $\text{mg g}^{-1}$ )	$K_L$ ( $\text{dm}^3 \text{mg}^{-1}$ )	$R_L$	$R^2$
0.4485	2.2296	7.8415	0.7254	60.2409	0.0703	0.1021	0.9596

### Kinetics studies

Various kinetics models in term of pseudo first, second order and intra particle diffusion were studied to examine the controlling mechanism of adsorption process. Pseudo first order kinetics model describe adsorption rate according to capacity of adsorption [48]. The pseudo first order kinetics model is represented in equation 4. The straight line was obtained when the plot is made between  $\log(q_e - q_t)$  and  $t$ . Its slope is represented  $-K_1/2.303$  and the intercept by  $\log q_e$  (Fig. 5a).

$$\log(q_e - q_t) = \log q_e - (K_1/2.303)t \quad \text{(Equation 4)}$$

In this equation,  $q_e$  represents amount of dye adsorbed at time  $t$  and  $q_t$ , amount of dye adsorbed at equilibrium.  $K_1$  represents rate constant.

Pseudo second order kinetics model was described by Ho and McKay for determination of kinetics of adsorption [49]. The equation 5 represents the linear equation of pseudo second order. A straight line is obtained by plotting  $t/q_t$  versus  $t$  with slope of  $1/q_e$  and intercept,  $K_2 q_e^2$  (Fig. 5b).

$$t/q_t = 1/K_2 q_e^2 + (1/q_e)t \quad \text{(Equation 5)}$$

Intra particle Diffusion is other kinetics model which was described by Weber and Morris for determination of the rate of adsorption of adsorbates molecule on adsorbent [50]. Linear form of the Intra particle Diffusion kinetics model is shown in Equation-6. The plot between  $q_t$  versus  $t^{1/2}$  gives a straight line which has the slope,  $K_d$  and intercept,  $C$  (Fig. 5c).

$$q_t = K_d t^{1/2} + C \quad \text{(Equation 6)}$$

The constant parameters of various kinetics models were given in Table 2. The correlation coefficient ( $R^2$ ) of Pseudo second order kinetics is 0.9950 that is well fitted as compared to Pseudo first order model ( $R^2 = 0.6813$ ) and Intra particle diffusion model ( $R^2 = 0.7413$ ). So, this means that pseudo second order kinetics is followed.

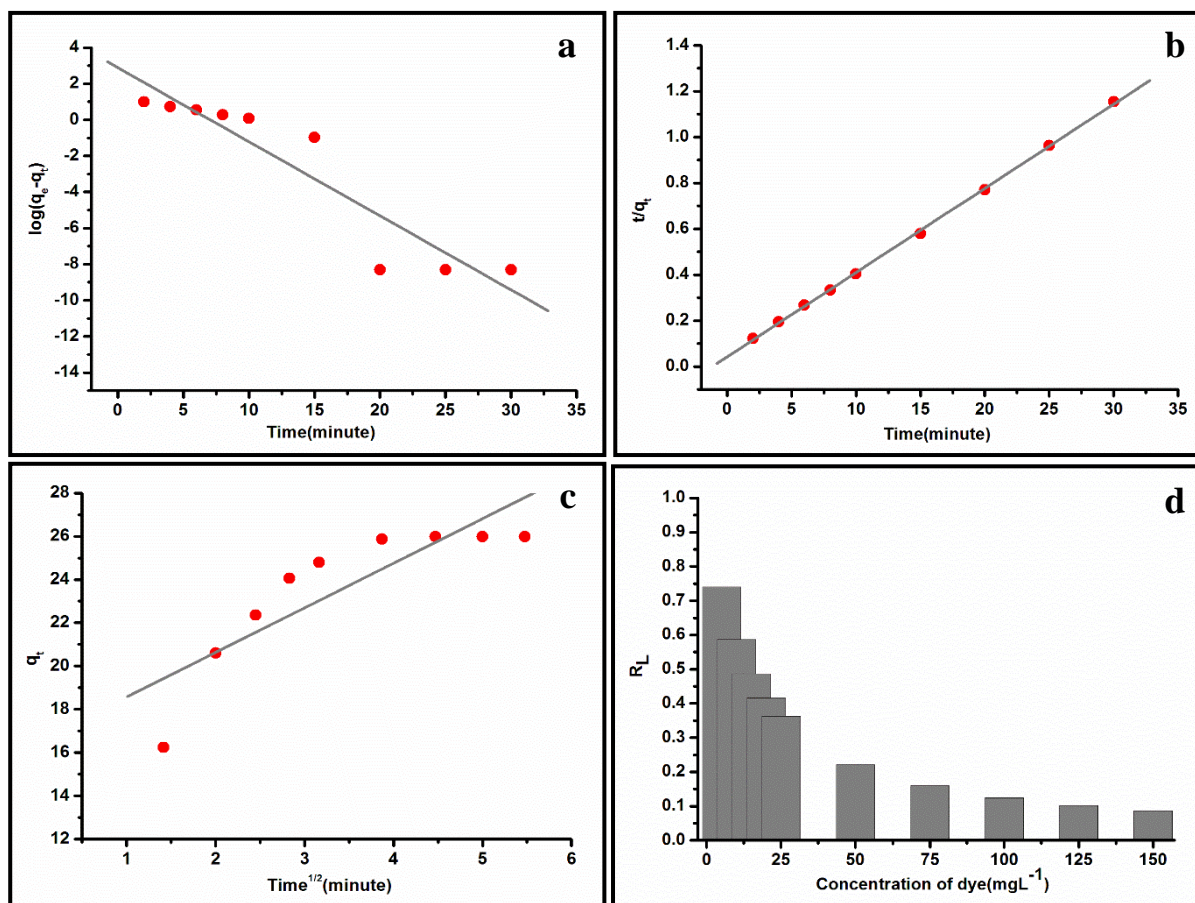


**Fig.5.** (a) Kinetics studies such as Pseudo first order (b) Pseudo second order (c) Intra particle diffusion and (d)  $R_L$  value

**Table 2.** Parameters constant of various kinetics models

Pseudo-first-order model			Pseudo-second-order model			Intraparticle diffusion model		
$K_1$	$q_e$	$R^2$	$K_2$	$q_e$	$R^2$	$K_d$	C	$R^2$
0.0610	3.6906	0.6813	0.0294	7.4239	0.9950	2.0619	16.513	0.7417

## Characterizations

### FTIR analysis

Fourier Transform Infrared spectrum of raw fly ash and the synthesized aluminosilicate (Hydroxysodalite) and RhB adsorbed HsL were recorded by Spectrum RXI Mid IR Perkin Elmer in the region  $400\text{-}4000\text{ cm}^{-1}$  (Fig. 6 and Fig. 7). In IR spectrum of raw fly ash, the presence of

quartz and mullite was shown by the peaks at  $1095\text{ cm}^{-1}$  and  $905\text{ cm}^{-1}$  [51-54]. The peaks at  $562\text{ cm}^{-1}$  and  $468\text{ cm}^{-1}$  is attributed to the presence of Si/Al ratio and tetrahedral unit ( $\text{TO}_4^{-4}$ ) in raw fly ash [55] (Fig. 6a).

The vibration bands at  $429\text{ cm}^{-1}$  and  $460\text{ cm}^{-1}$  appears in the spectrum of aluminosilicate (Hydroxysodalite) is linked to the band of absorption of the single four membering (S4R) and the bending band of O-T-O of the tetrahedron units ( $\text{TO}_4^{-4}$ ) (Fig. 6b). The adsorption bands in the region of  $900\text{-}1200\text{ cm}^{-1}$ ,  $550\text{-}800\text{ cm}^{-1}$ ,  $540\text{-}640\text{ cm}^{-1}$  and  $400\text{-}500\text{ cm}^{-1}$  are attributed to the presence S4R group resembling of zeolite [56].

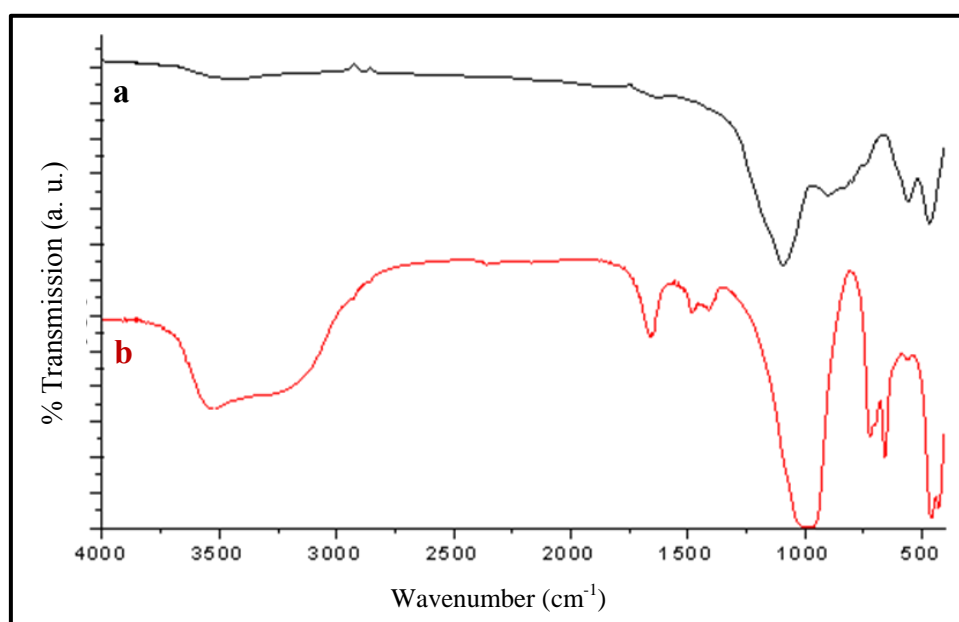


**Fig.6.** FTIR spectrums (a) Raw Fly ash (b) synthesized Hydroxysodalite

In the analysis of spectrum of adsorbed aluminosilicates, there is decrease in the peak in comparison to fly ash at the peak,  $562\text{ cm}^{-1}$  that means the dissolution of some amount of silica out of fly ash on formation of gel and that was decanted on washing of the product to reduce pH of the product. The symmetric and asymmetric stretching bands of T-O-T bond appeared at  $659\text{ cm}^{-1}$ ,  $702\text{ cm}^{-1}$  and  $988\text{ cm}^{-1}$  [57, 58]. The additional absorption bands at  $1411\text{ cm}^{-1}$  and  $1480\text{ cm}^{-1}$  appeared in the spectrum of the product is corresponding to  $\text{CO}_3^{-2}$  molecule trapped in the cavity of the hydroxysodalite [59, 60] and the absorption bands at  $1661\text{ cm}^{-1}$  and  $3280$

$\text{cm}^{-1}$  corresponds to the bending and stretching vibration band of Zeolitic water molecules of aluminosilicate. The additional bands appeared at  $3533 \text{ cm}^{-1}$  is because of Al-OH stretching bands of aluminosilicate. The frequencies of vibration appeared in spectrum of prepared product are similar to that of natural hydroxysodalite.

In case of RhB adsorbed Hydroxysodalite, there is additional adsorption band around  $1411 \text{ cm}^{-1}$  corresponding to  $-\text{CH}_2$  scissoring vibration of RhB. The peaks at  $1345 \text{ cm}^{-1}$  and  $1472 \text{ cm}^{-1}$  are due to CH vibration and  $1600 \text{ cm}^{-1}$  corresponds to C=O group of RhB. Absorption bands at  $1647 \text{ cm}^{-1}$  is because of  $\text{H}_2\text{O}$  bending vibration and the broad peak at  $3369 \text{ cm}^{-1}$  is due to presence of adsorbed and bonded water

The peak at  $978 \text{ cm}^{-1}$  is linked to the presence of Al-O-Si stretching bands of Hydroxysodalite. Presence of additional peaks of RhB dye in comparison to synthesized hydroxysodalite indicates adsorption of RhB on hydroxysodalite (Fig.7).

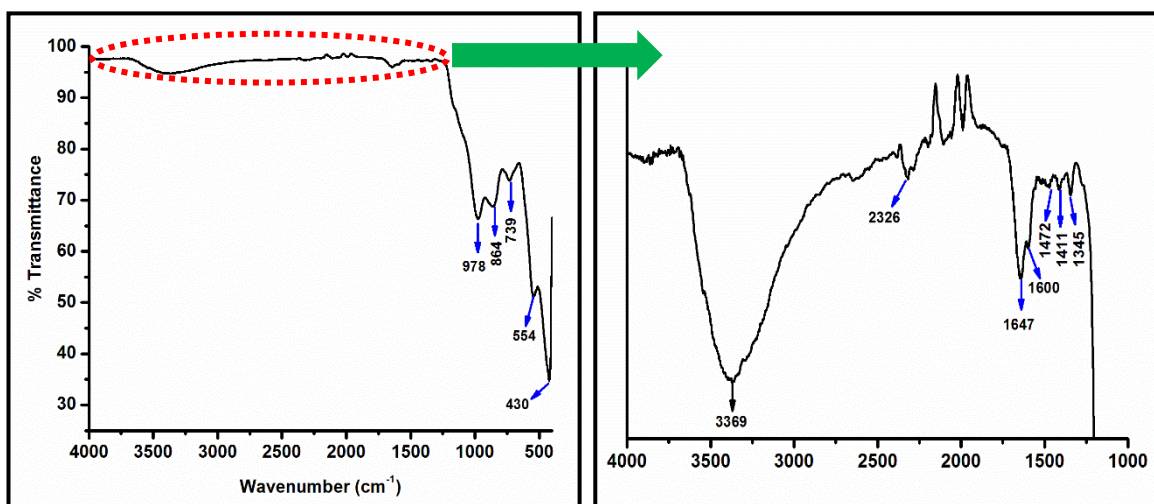


**Fig. 7.** FTIR spectrum of RhB adsorbed on Hydroxysodalite

### XRD analysis of Hydroxysodalite

Power X-ray diffraction (PXRD) pattern of raw fly ash and the synthesized aluminosilicate (Hydroxysodalite) were recorded between  $6$  to  $70^\circ$  ( $2\theta$ ) by X-ray Diffractometer (D8 DISCOVER BRUKER AXS, Germany) at  $40\text{kV}$  and  $30\text{mA}$  (Fig. 8).

In the XRD pattern of fly ash, the diffraction angle  $2\theta$  values are found to be 16.37, 20.87, 26.29, 31.04, 33.22, 35.31, 36.92, 39.23, 40.98, 42.58, 54.14, 57.72, 60.84 and 64.66. Broad hump around 26.29 and sharp intense peaks indicate that there is a mixture phase of amorphous and crystalline in fly ash (Fig. 8a).

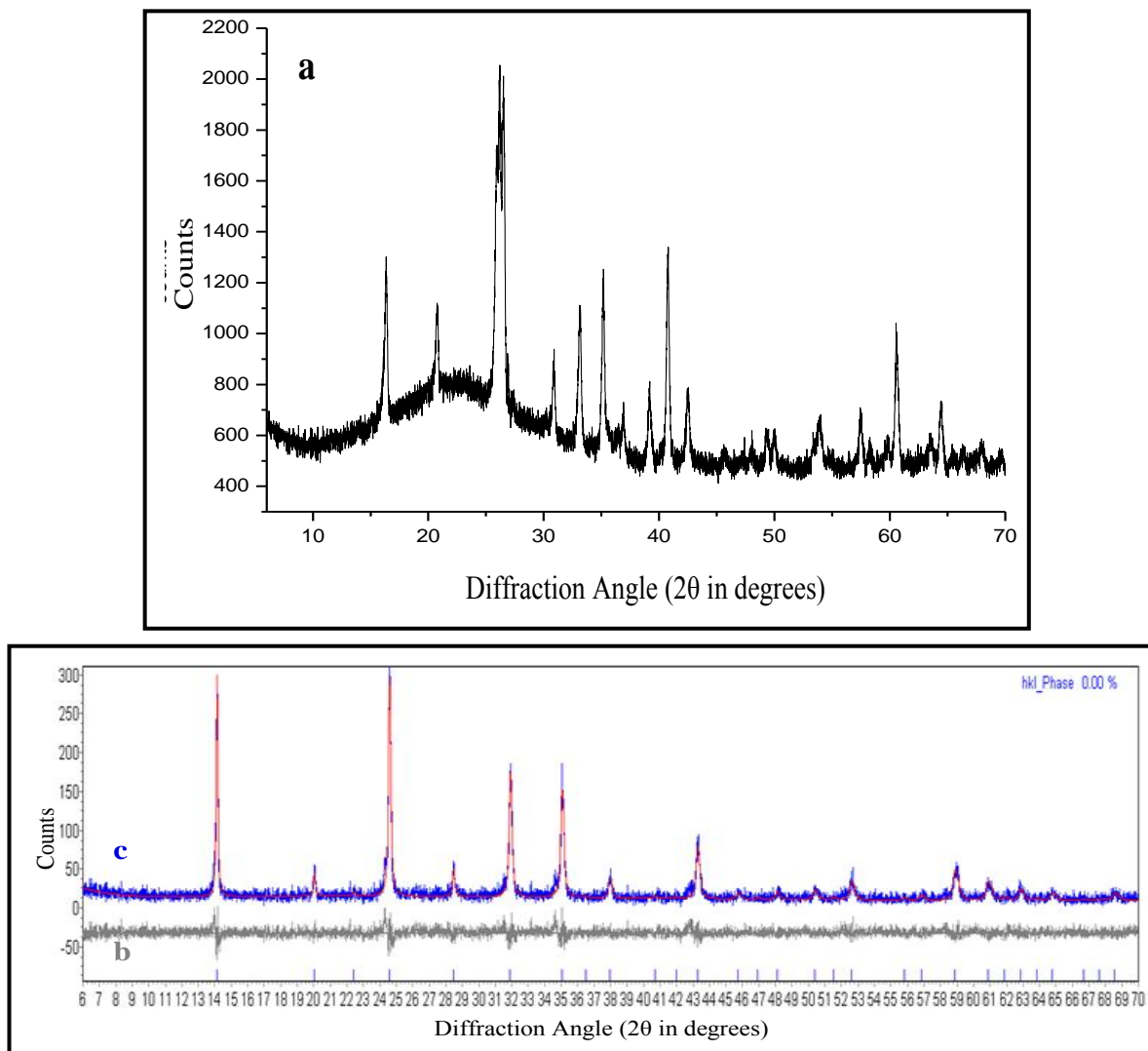


**Fig.8.**(a) XRD pattern of raw fly ash (b) vertical line on  $2\theta$  values denote the JCPDS-ICDD peak position (c) synthesized HsL

In case of synthesized HsL, diffraction angle  $2\theta$  values are found to be 14.06, 20.06, 24.56, 28.60, 31.96, 35.19, 38.08, 43.51, 45.82, 48.13, 50.66, 52.85, 57.03, 59.22, 61.18, 63.04, 65.00 and 68.93 (Fig. 8c). The synthesized product was analyzed with the help of Topas software. Disappearance of peaks in fly ash and reappearance of new sharp and intense peaks indicates the

formation of new framework aluminosilicate. In the synthesized product,  $2\theta$  positions for the diffraction peaks fit precisely to the  $\text{Na}_4\text{Al}_3\text{Si}_3\text{O}_{12}(\text{OH})$  composition cited by JCPDS-ICDD file No. 11-0401 (Hydroxysodalite phase with space group P-43n(218) in JCPDS-ICDD data) [61]. (Fig. 8b). The unit cell length of the product was calculated by analytical method using XRD  $2\theta$  values.

The relative intensities of the peaks in the synthesized product differ from that of naturally occurring HsL indicating difference in the Si/Al ratio. An increase in the unit cell length of the synthesized product from that of naturally occurring HsL indicates decrease in the Si/Al ratio or crystal defect due to the presence of impurities in the synthesized HsL. The peak positions in the synthesized product were found to be in good agreement with the peaks of Hydroxysodalite.

### **TGA analysis of Hydroxysodalite**

Thermogravimetric analysis (TGA) pattern of the synthesized HsL were recorded between 30 to 750 °C by TECNAI G2T30FEL (Fig. 9). Synthesized HsL shows four stages of weight losses between 30 to 750 °C i.e.; first weight loss between 30 to 147.17°C is 5.12% that indicates moisture losses, Second weight loss between 147.17°C to 237 °C is 5.55 % which is due to desorption of physically adsorbed water out of micropores, third weight loss between 237 °C to 286.29 °C is 2.19% that is considered to be linked to loss of water out of hydration complexes formed with exchangeable cation [62] and fourth weight loss in between 286.29 °C to 750 °C is of 1.67% which is due to dehydroxylation and destruction of hydroxyl bonds formed [63].

TGA curve of the synthesized compound shows total weight loss of 13.59% from 37.49 °C to 627.78 °C (Fig. 9a). The DTA curve shows two endothermic peaks, the first endothermic peaks at 147.3 °C corresponding to the dehydration of the adsorbed surface water molecules and second, endothermic peak at 236 °C corresponding to the dehydration of Zeolitic water molecules (Fig. 9b).

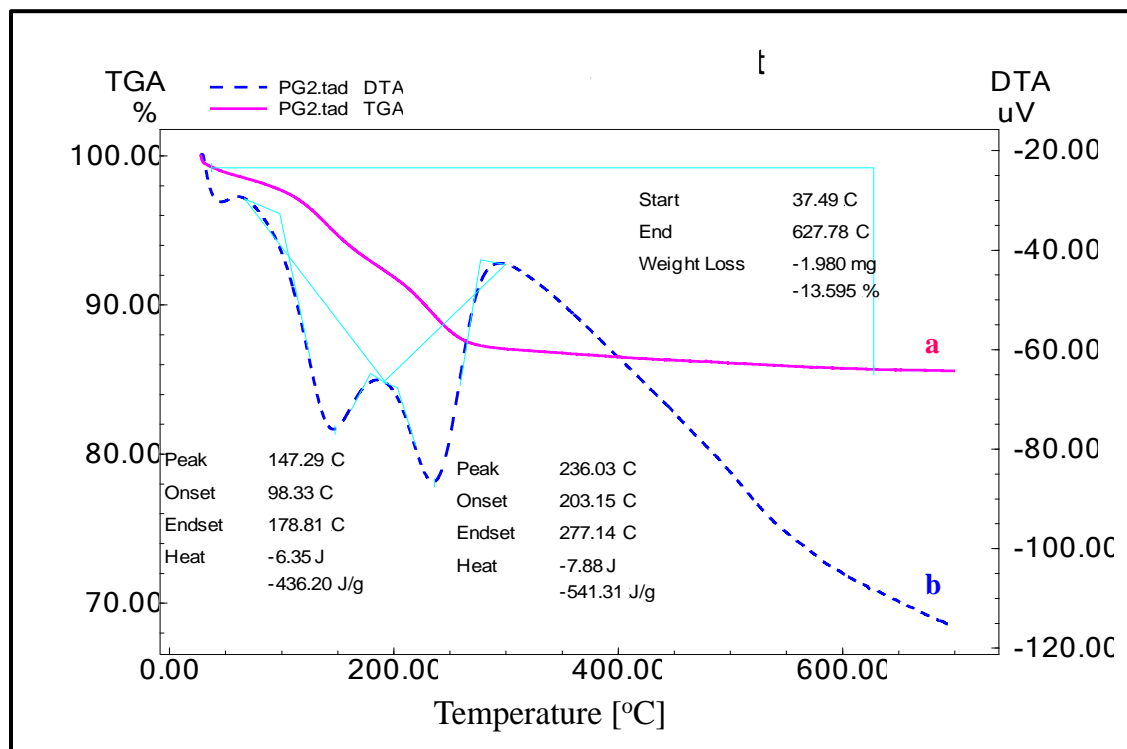


**Fig.9.** Smooth line represents the TGA curve (a) and dotted line, the DTA curve (b) of synthesized hydroxysodalite

### SEM and TEM analysis of Hydroxysodalite

Scanning Electron Microscopic (SEM) and Transmission Electron Microscopic (TEM) image of synthesized HsL were recorded using JEOL JSM-6610LV and TECNAI G2T30FEL respectively (Fig.10, Fig.11). SEM of the RhB adsorbed hydroxysodalite (Fig. 12).

The SEM image of synthesized HsL shows unique hierarchical spherical and disc-like platelets. Size of the disc-like platelets is in the range of 40 nm to 90 nm (Fig. 10a to 10c). EDS analysis of the synthesized aluminosilicate indicates negligible amount of heavy metals such as Fe, Ti, Mg, Ca and Cr etc.. The atomic ratio of Si/Al in the synthesized product calculated from EDS is slightly less than unity (Fig. 10d). TEM images show unique hierarchical spherical and slightly cubical platelets of synthesized HsL. Size of the spherical platelets is in between 50 nm to 180 nm (Fig. 11a to 11e).

The shapes of the nano size crystal are observed to be cubical. EDX confirmed that synthesized product is alumina rich rather than silica-rich and presence of some heavy metal ions, such as Fe,



Ti, Mg, Ca that might have replaced silicon atoms in the frame work structure. Presence of bright spots in diffraction pattern indicates the product as crystalline in nature (Fig. 11f).

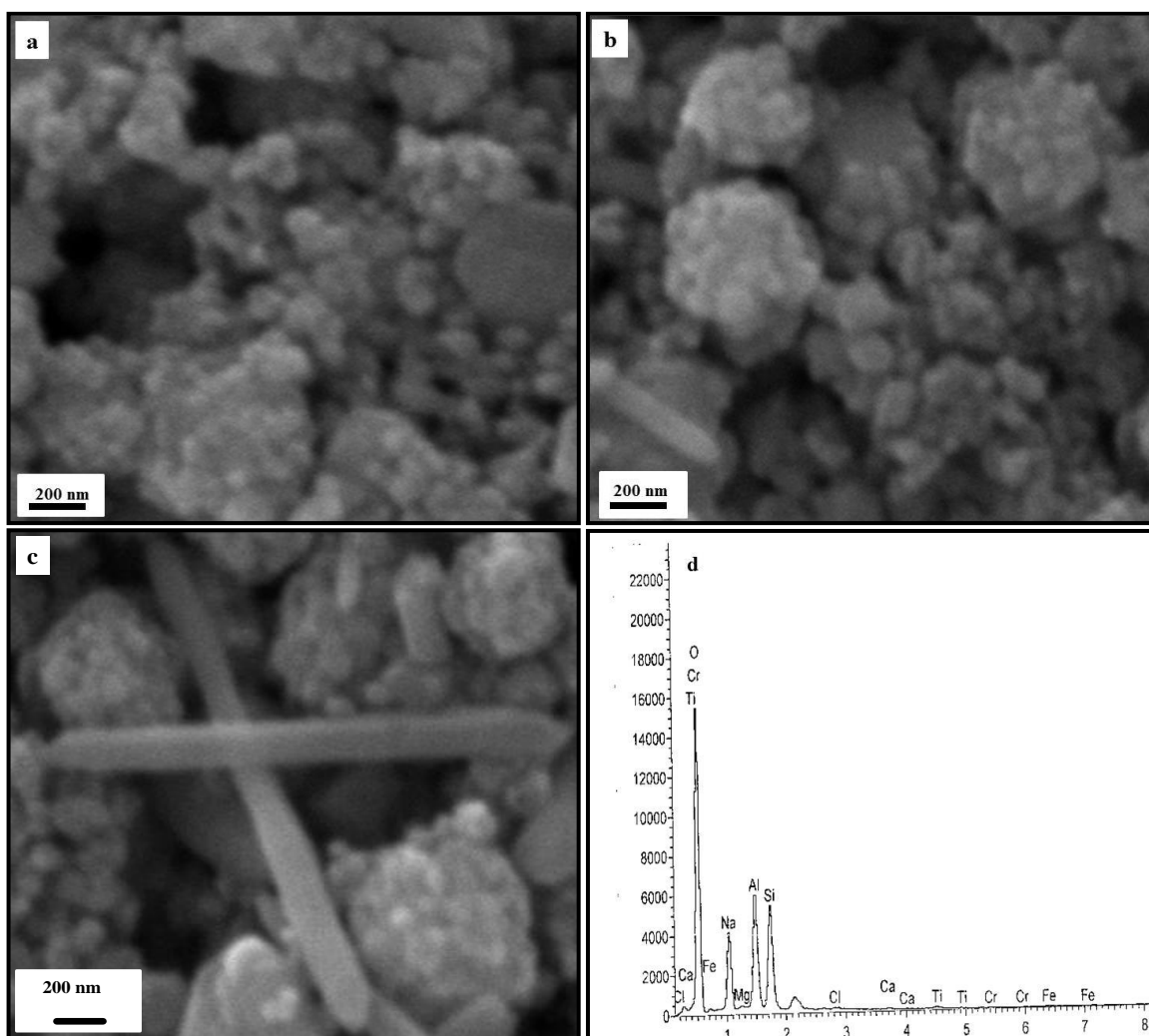


**Fig.10.** (a), (b) & (c) SEM images of synthesized HsL with different magnification and (d) EDS plot of synthesized HsL

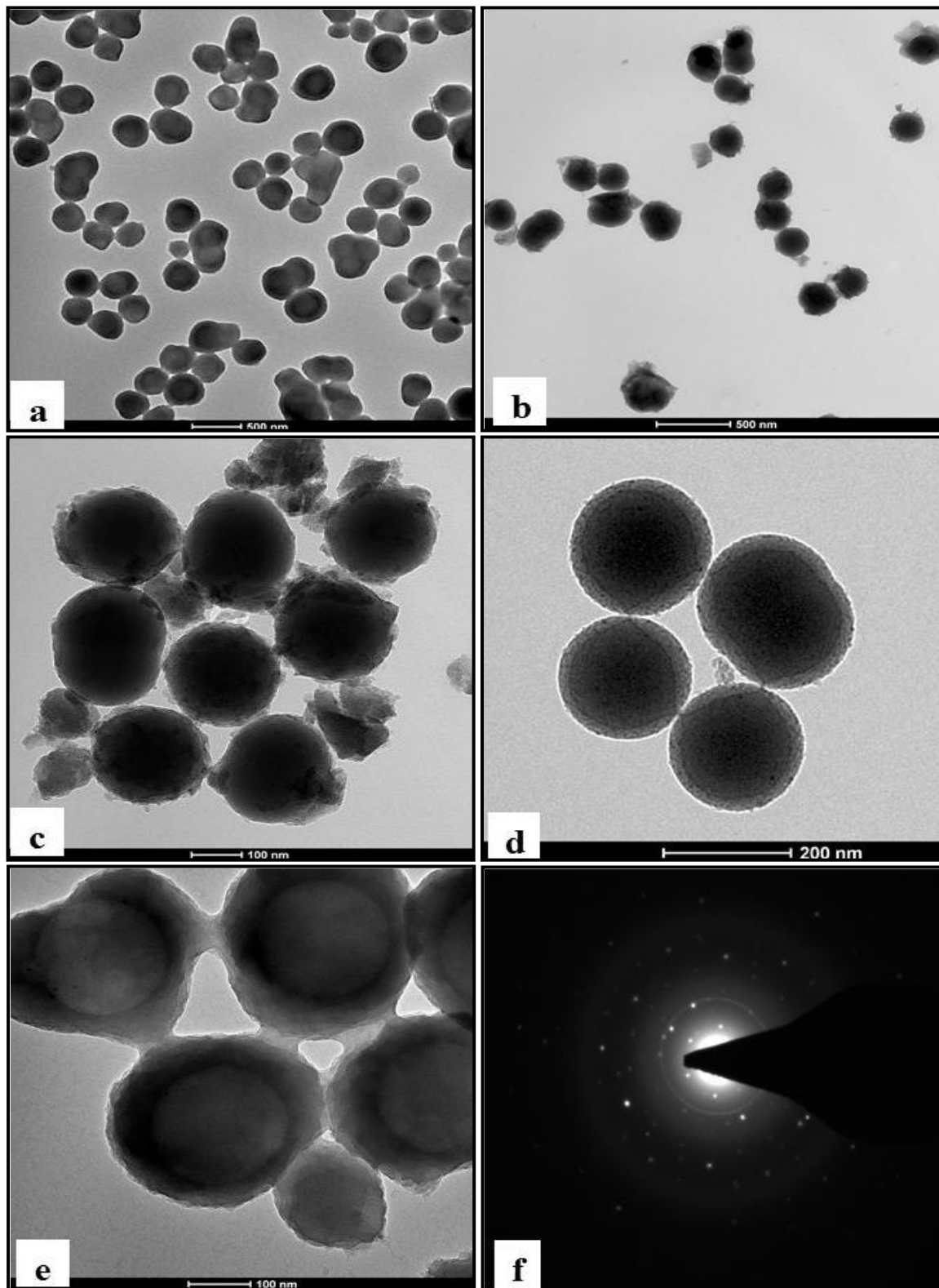


**Fig.11.**(a), (b), (c), (d) & (e) TEM images of synthesized HsL with different magnification and (f) EDX pattern of synthesized HsL

The SEM image of RhB adsorbed on HsL was relatively smooth as compared to that of pristine HsL. Size of the RhB adsorbed on HsL is in between 2 to 4  $\mu$  with spherical shape (Fig. 12a-12c). In case of EDS analysis of the RhB adsorbed on HsL shows the presence of heavy metals such as C, N, O, Al, Si, etc. The presences of Carbon peak (from RhB dye) indicates RhB dye adsorbed on hydroxysodalite (Fig. 12d).

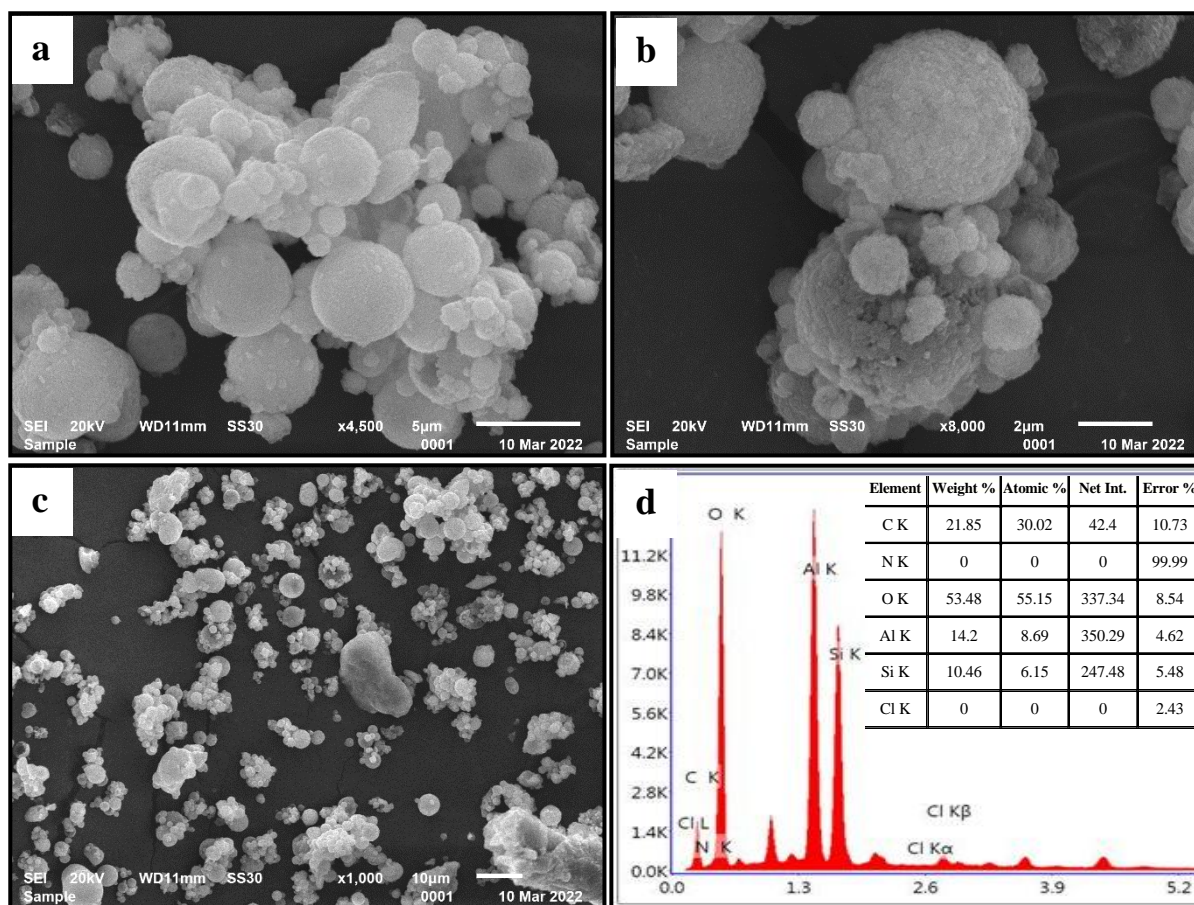


**Fig. 12.**(a), (b) & (c) SEM images of RhB adsorbed on HsL(d) EDS plot of elemental composition present in RhB adsorbed on HsL

### Interaction of RhB dye with HsL in adsorption

In the adsorption process, HsL has some adsorptive site that interacts with RhB dye, possible schematic diagram of mechanism of interaction between HsL with RhB(Fig.13).RhB dye adsorbed on the surface of HsL due to because of electrostatic interaction and some molecule are also trapped inside the pores of HsL[64, 65].

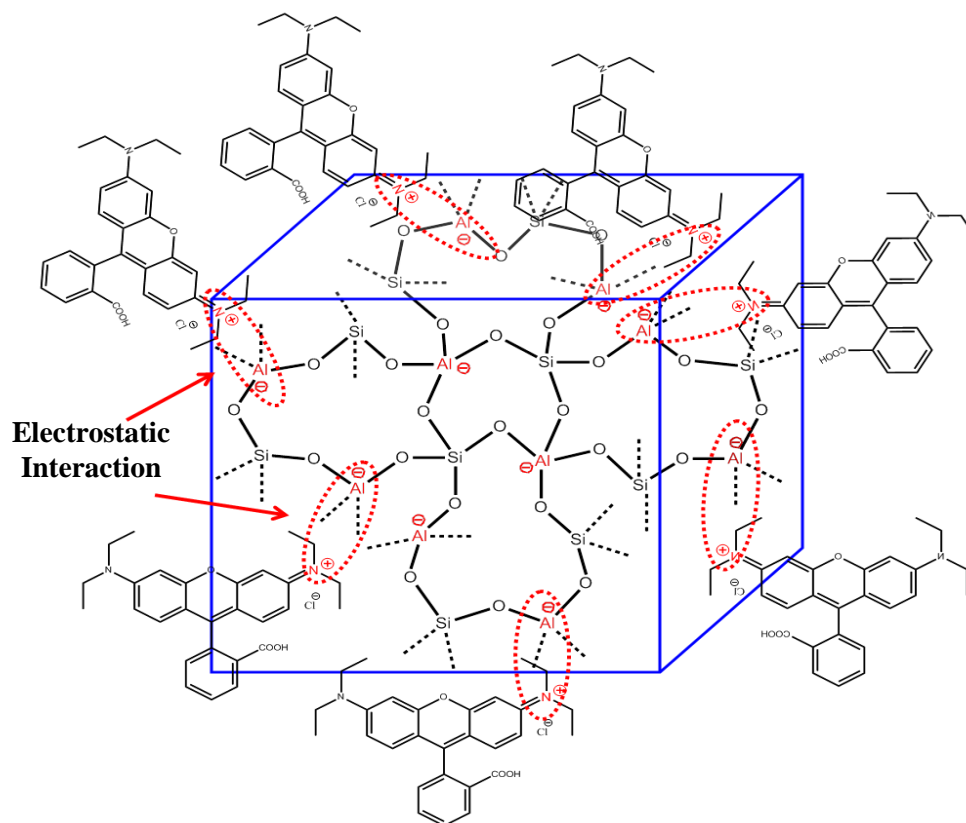


**Fig.13.** Schematic diagram of interaction between HsL with RhB

### Conclusion

The synthesis of HsL by hydrothermal method from waste fly ash was successfully performed in two step process and the synthesized products were characterized by TEM, SEM and FTIR. Unique hierarchical spherical and disc-like platelets with size of 40 nm to 180 nm were displayed in SEM and TEM images. TGA curve of synthesized compound shows total weight loss of 13.59% from 37.49 °C to 627.78 °C. The peak positions of XRD and FTIR in the synthesized product were found to be in good agreement with the peaks of HsL. Adsorption parameters of dye adsorbed on HsL observed from batch studies adsorption isotherms and kinetics models reveals that the process involved follows Langmuir adsorption mechanism and kinetic of Pseudo second order. The highest remediation of RhB was found to be 1032.48 μg at 125 ppm concentration, and  $R_L$  value less than 1 confirms the involvement of favorable adsorption process. It is also observed that the interaction between the dye and HsL is of electrostatic in

nature with trapping of molecules inside the pores of HsL. Therefore, the synthesized HsL is a potential material in remediation of RhB dye out of aqueous solution. Therefore, it is concluded that the study is significant for restoration of the natural resources like water, air and agricultural lands from pollution of fly ash as well as from RhB dye.

### **Conflict and Interest**

There is no conflict of interest regarding manuscript that is declared by the authors.

### **Acknowledgements**

The authors are indebted to the head of Kirori Mal, University of Delhi for encouraging and supporting for the research work.

### **Reference**

- [1] S. Golbad, P. Khoshnoud, N. Abu-Zahra, Hydrothermal synthesis of hydroxysodalite from fly ash for the removal of lead ions from water, *Int. J. Environ. Sci. Technol.* 14 (2017), 135–142. doi:10.1007/s13762-016-1133-x
- [2] D. D. Kragten, N. C Burnsville, Preparation of hydroxysodalite, United States Patent Application Publication Kragten, Pub. No.: US 2007/0237700 A1, Oct. 11, (2007), 1-7.
- [3] B. Liu, H. Sun, T. Peng, Q. He, One-step synthesis of hydroxysodalite using natural bentonite at moderate temperatures, *Minerals* 8 (521) (2018) 2-14. <https://doi.org/10.3390/min8110521>
- [4] J. Yao, L. Zhang, H. Wang, Synthesis of nanocrystalline sodalite with organic additives, *Mater. Lett.* 62 (2008), 4028–4030. <https://doi.org/10.1016/j.matlet.2008.05.053>
- [5] M. K. Naskar, D. Kundu, M. Chatterjee, Effect of process parameters on surfactant-based synthesis of hydroxysodalite particles, *Mater. Lett.* 65 (2011), 436–438. <https://doi.org/10.1016/j.matlet.2010.11.008>
- [6] I. Hassan, H. D. Grundy, The crystal structures of sodalite-group minerals, *Acta Crystallographica Section B.* 40 (1984) 6–13. <https://doi.org/10.1107/S0108768184001683>
- [7] M. Kazemimoghdam, Z. A. Rigi, Evaluation and synthesis of Nano-pore Hydroxysodalite (HS) zeolite membranes: Application to pervaporation of Ethanol/water mixture, *J. Water Environ. Nanotechnol.* 3(2) Spring (2018), 173-190. Doi: 10.22090/JWENT.2018.02.008
- [8] S. G. Sorenson, E. A. Payzant, W. T. Gibbons, B. Soydas, H. Kita, R. D. Noble, Influence of zeolite crystal expansion/ contraction on NaA zeolite membrane separations, *Journal of Membrane Science.* 366(1-2) (2011), 413-20. <https://doi.org/10.1016/j.memsci.2010.10.043>

- [9] G. Liu, Z. Jiang, K. Cao, S. Nair, X. Cheng, J. Zhao, Pervaporation performance comparison of hybrid membranes filled with two-dimensional ZIF-L nanosheets and zero-dimensional ZIF-8 nanoparticles, *Journal of Membrane Science* 523 (2017), 185-196.  
Doi:10.1016/j.memsci.2016.09.064
- [10] C. Zhou, Q. Gao, W. Luo, Q. Zhou, H. Wang, C. Yan, P. Duan, Preparation characterization and adsorption evaluation of spherical mesoporous Al-MCM-41 from coal fly ash, *J. Taiwan Inst. Chem. Eng.* 52 (2015) 147–157. DOI:10.1016/j.jtice.2015.02.014
- [11] M. Franus, M. Wdowin, L. Bandura, W. Franus, Removal of environmental pollutions using zeolites from fly ash: a review. *J. Fresenius Environ. Bull.* 24 (2015), 854–866.
- [12] H. L. Chang, C. M. Chun, I. A. Aksay, W. H. Shih, Conversion of fly ash into mesoporous aluminosilicate, *J. Ind. Eng. Chem. Res.* 38(3) (1999) 973–977. Doi: 10.1021/ie980275b
- [13] S. Golbad, P. Khoshnoud, N. Abu-Zahra, Hydrothermal synthesis of hydroxysodalite from fly ash for the removal of lead ions from water, *Int. J. Environ. Sci. Technol.* 14 (2017), 135–142. DOI: [10.1007/s13762-016-1133-x](https://doi.org/10.1007/s13762-016-1133-x)
- [14] R. L. Aitken, L. C. Bell, Plant uptake and phytotoxicity of boron in Australian fly ash, *Journal of Plant and Soil* 84 (1985), 245-257. <https://doi.org/10.1007/BF02143187>
- [15] S. V. Mattigod, D. Rai, L. E. Eary, C. C. Ainsworth, Geochemical factors controlling the mobilization of inorganic constituents from fossil fuel combustion residues: review of the major elements, *Journal Environmental Quality*, 19 (1990), 188-201. <https://doi.org/10.2134/jeq1990.00472425001900020004x>
- [16] C. C. Yuan, W. C. Fang, D. T. Mui, H. L. Chiang, Application of methods (sequential extraction procedures and high-pressure digestion method) to fly ash particles to determine the elements: a case study of BCR 176, *J. Hazard. Mater.* 163 (2009) 578-587.  
DOI: 10.1016/j.jhazmat.2008.07.039
- [17] A. Dwivedi, M. K. Jain, Fly ash – waste management and overview: A Review, *Recent Research in Science and Technology*, 6(1) (2014), 30-35.
- [18] C. F. Wang, L. J. Sheng, W. L. Jun, S. X. Yun, Influence of NaOH concentrations on synthesis of pure form Zeolite A from fly ash using two-stage method, *J Hazard Mater.* 155 (2008), 58-64. DOI: 10.1016/j.jhazmat.2007.11.028

- [19] A. Derkowski, W. Franus, B. Elzbieta, A. Czimerova, Properties and potential applications of Zeolitic materials produced from fly ash using simple method of synthesis, *Powder Technology* 166 (2006), 47-54.
- [20] N. Murayama, H. Yamamoto, J. Shibata, Mechanism of zeolite synthesis from coal fly ash by alkali hydrothermal reaction, *Int. J. Miner. Process.* 64 (2002) 1-17. DOI:10.1016/S0301-7516(01)00046-1
- [21] V. K. Gupta, I. Ali, Adsorbents for water treatment: Low-cost alternatives to carbon, *Encyclopaedia of surface and colloid science*, Edited by Ponisseril Somasundaran, Marcel Dekker, New York, USA, (2003), 1-34.
- [22] N. Ghazali, K. Muthusamy, S. W. Ahmad, Utilization of fly ash in construction, *IOP Conf. Series: Materials Science and Engineering* 601 (2019), 012023. doi:10.1088/1757-899X/601/1/012023
- [23] K. A. Adegoke, R. O. Oyewole, B. M. Lasisi, O. S. Bello, Abatement of organic pollutants using fly ash based adsorbents, *Water Sci. Technol.* 76 (2017) 2580–2592. DOI: [10.2166/wst.2017.437](https://doi.org/10.2166/wst.2017.437)
- [24] A. Kant, M. R. Singh, S. Ghosh, P. Gajon, Synthesis of valuable transition metal incorporated framework aluminosilicates using waste material fly ash, *ChemSci Rev Lett*, 8 (32) (2019), 302-308.
- [25] T. Henmi, Chemical conversion of coal ash into artificial zeolite and its recycling, *New Ceram*, 7 (1997), 54-62.
- [26] S. E. Aprianti, A huge number of artificial waste material can be supplementary cementitious material (SCM) for concrete production – A review part II, *J. Clean. Prod.* 142 (2017), 4178–4194.
- [27] S. Hsu, M. Chi, R. Huang, Effect of fineness and replacement ratio of ground fly ash on properties of blended cement mortar, *Constr. Build. Mater.* 176 (2018) 250–258. DOI: [10.1016/j.conbuildmat.2018.05.060](https://doi.org/10.1016/j.conbuildmat.2018.05.060)
- [28] R. K. Anjani, V. V. Gollakota, C. M. Shu, Progressive utilisation prospects of coal fly ash: a review, *Sci. Total Environ.* 672 (2019) 951–989. DOI: [10.1016/j.scitotenv.2019.03.337](https://doi.org/10.1016/j.scitotenv.2019.03.337)
- [29] A. Bhatt, S. Priyadarshini, A. A. Mohanakrishnan, A. Abri, M. Sattler, S. Techapaphawit, Case Studies in Construction Materials Physical, chemical, and geotechnical properties of coal fly ash: A global review, *Case Studies in Construction Materials* 11 (2019), e00263.

- [30] U. S. Geological Survey, Radioactive Elements in Coal and Fly ash. Abundance, Forms and Environmental Significance, U. S. Geological Survey Fact SHEET FS - (1997), 163-197.
- [31] M. Xiangju, N. Faisal, X. F. Shou, Templating route for synthesizing mesoporous zeolites with improved catalytic properties, *Nano Today* 4 (2009), 292-301.
- [32] C. J. H. Jacobsen, C. Madsen, J. Houzvicka, I. Schmidt, A. Carlsson, Mesoporous Zeolite Single Crystals, *J. Am. Chem. Soc.* 122, (2000), 7116-7117. <https://doi.org/10.1021/ja000744c>
- [33] C. F. Lin, H. C. His, Resource recovery of waste fly ash: synthesis of zeolite-like materials. *J Environ Sci Technol.* 29 (4) (1995), 1109–1117. DOI: [10.1021/es00004a033](https://doi.org/10.1021/es00004a033)
- [34] S. Senguttuvan, P. Senthilkumar, V. Janaki and S Kamala-Kanman. Significance of conducting polyaniline based composites for the removal of dyes and heavy metals from aqueous solution and waste water-A Review. *Chemosphere*. 267 (2021), 129201. DOI: [10.1016/j.chemosphere.2020.129201](https://doi.org/10.1016/j.chemosphere.2020.129201)
- [35] C. P. Sekhar, S. Kalidhasan, V. Rajesh, N. Rajesh. Bio-polymer adsorbent for the removal of malachite green from aqueous solution. *Chemosphere* 77 (2009), 842-847. DOI: [10.1016/j.chemosphere.2009.07.068](https://doi.org/10.1016/j.chemosphere.2009.07.068)
- [36] A. Yadav, N. Bagotia, S. Yadav, A. K. Sharma. Adsorptive studies on the removal of dyes from single and binary systems using saccharummunja plant-based novel functionalized CNT composites. *Environmental Technology & Innovation* 24 (2021), 102015. <https://doi.org/10.1016/j.eti.2021.102015>
- [37] L. Ai, C. Zhang, L. Meng, Adsorption of Methyl Orange from Aqueous Solution on Hydrothermal Synthesized Mg-Al Layered Double Hydroxide. *J. Chem. Eng. Data.* 56 (2011), 4217–4225. <https://doi.org/10.1021/jc200743u>
- [38] Z. Li, B. Ma, X. Zhang, Y. Sang, H. Liu, One-pot synthesis of BiOCl nanosheets with dual functional carbon for ultra-highly efficient photocatalytic degradation of RhB. *Environ. Res.* 182 (2020), 109077. DOI: [10.1016/j.envres.2019.109077](https://doi.org/10.1016/j.envres.2019.109077)
- [39] G. Kumar and D. T. Masram, Sustainable Synthesis of MOF-5@GO Nanocomposites for Efficient Removal of Rhodamine B from Water, *ACS Omega* 6 (2021), 9587–9599. [Doi.org/10.1021/acsomega.1c00143](https://doi.org/10.1021/acsomega.1c00143)
- [40] N. Y. Usachev, E. P. Belanova, L. M. Krukovsky, S. A. Kanaev, O. K. Ataloyan, A. V. Kazakov, Thermal transformations in systems based on zeolites Y, X, and A containing zinc and



sodium nitrates. *Russ. Chem. Bull.* 52 (2003), 1940–1949.

DOI: [10.1023/B:RUCB.0000009636.89718.56](https://doi.org/10.1023/B:RUCB.0000009636.89718.56)

[41] M. Kaur, M. Datta. Adsorption Equilibrium and Kinetics of Toxic Dye-Erythrosine B Adsorption onto Montmorillonite. *Separation Science and Technology*. 48 (2013), 1370–1381. DOI: [10.1080/01496395.2012.727939](https://doi.org/10.1080/01496395.2012.727939)

[42] T. H. Vermeulan, K. R. Vermeulan, Hall LC Fundamental. *Indian Engineering Chemistry* 5 (1966), 212–223.

[43] A. Kant, P. Gaijon and U. Nadeem, Adsorption Equilibrium and Kinetics of Crystal Violet Dye from Aqueous Media onto Waste Material, *ChemSci Rev Lett*. 3(11S) (2014), 1-13.

[44] S. J. Allen, G. McKay, J. F. Porter. Adsorption isotherm models for basic dye adsorption by peat in single and binary component systems. *J Colloid Interface Sci.* 280(2004), 322–333.

DOI: [10.1016/j.jcis.2004.08.078](https://doi.org/10.1016/j.jcis.2004.08.078)

[45] E. Demirbas, M. Kobya, Konukman AES. Error analysis of equilibrium studies for the almond shell activated carbon adsorption of Cr(VI) from aqueous solutions. *J Hazard. Mater.* 154(2008), 787–794. <https://doi.org/10.1016/j.jhazmat.2007.10.094>

[46] U. Nadeem, A. Kant & P. Gaijon, Equilibrium And Kinetics Studies For The Adsorption Of Crystal Violet Dye By *Spirulina Platensis*, *International Journal of Applied and Natural Sciences*. 3 (5) (2014), 9-20.

[47] T. W. Webber, R. K. Chakravorti. Pore and solid diffusion models for fixed bed adsorbers. *AIChE J*; 20 (1974), 228–238. DOI: [10.1002/AIC.690200204](https://doi.org/10.1002/AIC.690200204)

[48] Lagergren S. About the theory of so called adsorption of soluble substances. *Handlingar Band.* 24(1898), 1-39.

[49] G. L. Dotto, E. C. Lima, L. A. A. Pinto. Biosorption of food dyes onto *Spirulina platensis* nanoparticles: equilibrium isotherm and thermodynamic analysis. *Bioresour Technol* 103 (2012), 123–130. DOI: [10.1016/j.biortech.2011.10.038](https://doi.org/10.1016/j.biortech.2011.10.038)

[50] W. J. Weber, J. C. Morris. Kinetics of adsorption on carbon from solution, *Eng. Div. Proceed. Am. Soc. Civil. Eng.* 89 (1963), 31–60.

[51] P. Padmaja, G. M. Anilkumar, P. Mukundan, G. Aruldas, K. G. K. Warriar, Characterisation of stoichiometric sol-gel mullite by fourier transform infrared spectroscopy, *International Journal of Inorganic Materials* 3 (2001), 127-130.

- [52] M. Daniel, D. N. Y. Ilhan, Nanocomposite mullite/mullite powders by spray pyrolysis, *Journal of Nanoparticle Research* 1 (1999), 127-130.
- [53] D. R. Treadwell, D. M. Dabbs and I. A. Aksay, Mullite ( $3\text{Al}_2\text{O}_3\text{-SiO}_2$ ) synthesis with aluminosiloxanes, *Chem. Mater.* 8 (1996), 2056-2060.
- [54] M. A. Virji, D. Bello, S. R. Woskie, X. M. Liu, A. J. Kalil, Analysis of quartz by FTIR in air samples of construction dust, *Applied occupational and environmental hygiene.* 17 (3) (2002), 165-175. doi: 10.1080/104732202753438252.
- [55] A. J. M. D. Man and R. A. V. Santen, The relation between zeolite framework and vibrational spectra, *Zeolites*, 12 (1992) 269-279. [https://doi.org/10.1016/0144-2449\(92\)90100-4](https://doi.org/10.1016/0144-2449(92)90100-4), [https://doi.org/10.1016/S0144-2449\(05\)80295-7](https://doi.org/10.1016/S0144-2449(05)80295-7)
- [56] M. Wlodzimierz, K. Magdalena, B. Katarzyna, FT-IR studies of zeolites from different structural Groups, *CHEMIK*, 65 (7) (2011) 667-674.
- [57] C. M. B. Henderson, D. Taylor, Infrared spectra of anhydrous members of the sodalite family, *Spectrochimica Acta*, 33A (1977), 283-290. [https://doi.org/10.1016/0584-8539\(77\)80032-9](https://doi.org/10.1016/0584-8539(77)80032-9)
- [58] B. I. Shikunov, L. I. Lafer, V. I. Yakerson, I. V. Mishin, A. M. Rubinshtein, Infrared spectra of synthetic zeolites, *UDC* 543.422.4:541.183:549.67. doi:10.1007/bf00855697
- [59] K. Hadjiivanov, E. Ivanova, H. Knozinger, FTIR study of low-temperature CO adsorption on Y zeolite exchanged with  $\text{Be}^{2+}$ ,  $\text{Mg}^{2+}$ ,  $\text{Ca}^{2+}$ ,  $\text{Sr}^{2+}$  and  $\text{Ba}^{2+}$  cations, *Microporous and Mesoporous Materials*, 58 (2003), 225-236. [https://doi.org/10.1016/S1387-1811\(02\)00650-9](https://doi.org/10.1016/S1387-1811(02)00650-9)
- [60] G. Busca, V. Lerezelli, Infrared spectroscopic identification of species arising from reactive adsorption of carbon dioxides on metal oxide surfaces, *Materials Chemistry*, 7 (1982), 89-126. DOI:10.1016/0390-6035(82)90059-1
- [61] JCPDS-ICDD File No. 11-0401.
- [62] N. Y. Usachev, E. P. Belanova, L. M. Krukovsky, S. A. Kanaev, O. K. Ataloyan, A. V. Kazakov, Thermal transformations in systems based on zeolites Y, X, and A containing zinc and sodium nitrates. *Russ. Chem. Bull.* 52 (2003) 1940–1949.
- [63] S. Akbar, K. Dad, T. H. Shah, R. Shahnaz, Thermal studies of NaX zeolite with different degrees of cadmium exchange. *J. Chem. Soc. Pak.* 27 (2005) 456–461.
- [64] Y. Yua, B. N. Murthya, J. G. Shaptera, K. T. Constantopoulou, N. H. Voelckerb, A. V. Ellis. Benzene carboxylic acid derivatized graphene oxide nanosheets on natural zeolites as

effective adsorbents for cationic dye removal. *J. Hazard. Mater.* 260 (2013), 330–338. <http://dx.doi.org/10.1016/j.jhazmat.2013.05.041>

[65] H. Mittal, S. B. Mishra. Gum ghatti and Fe<sub>3</sub>O<sub>4</sub> magnetic nanoparticles-based nanocomposites for the effective adsorption of rhodamine B. *Carbohydr. Polym.* 101 (2014) 1255–1264. DOI: [10.1016/j.carbpol.2013.09.045](https://doi.org/10.1016/j.carbpol.2013.09.045)